SUPPLEMENTARY FIGURES

Fig. 1S-A

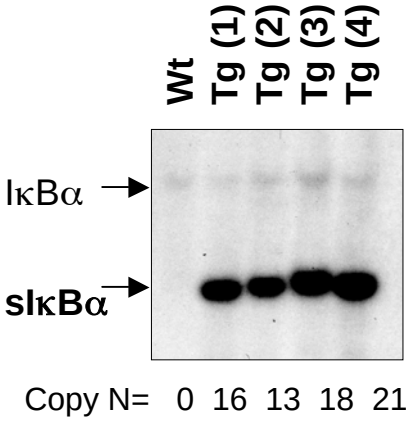

Fig. 1S-B

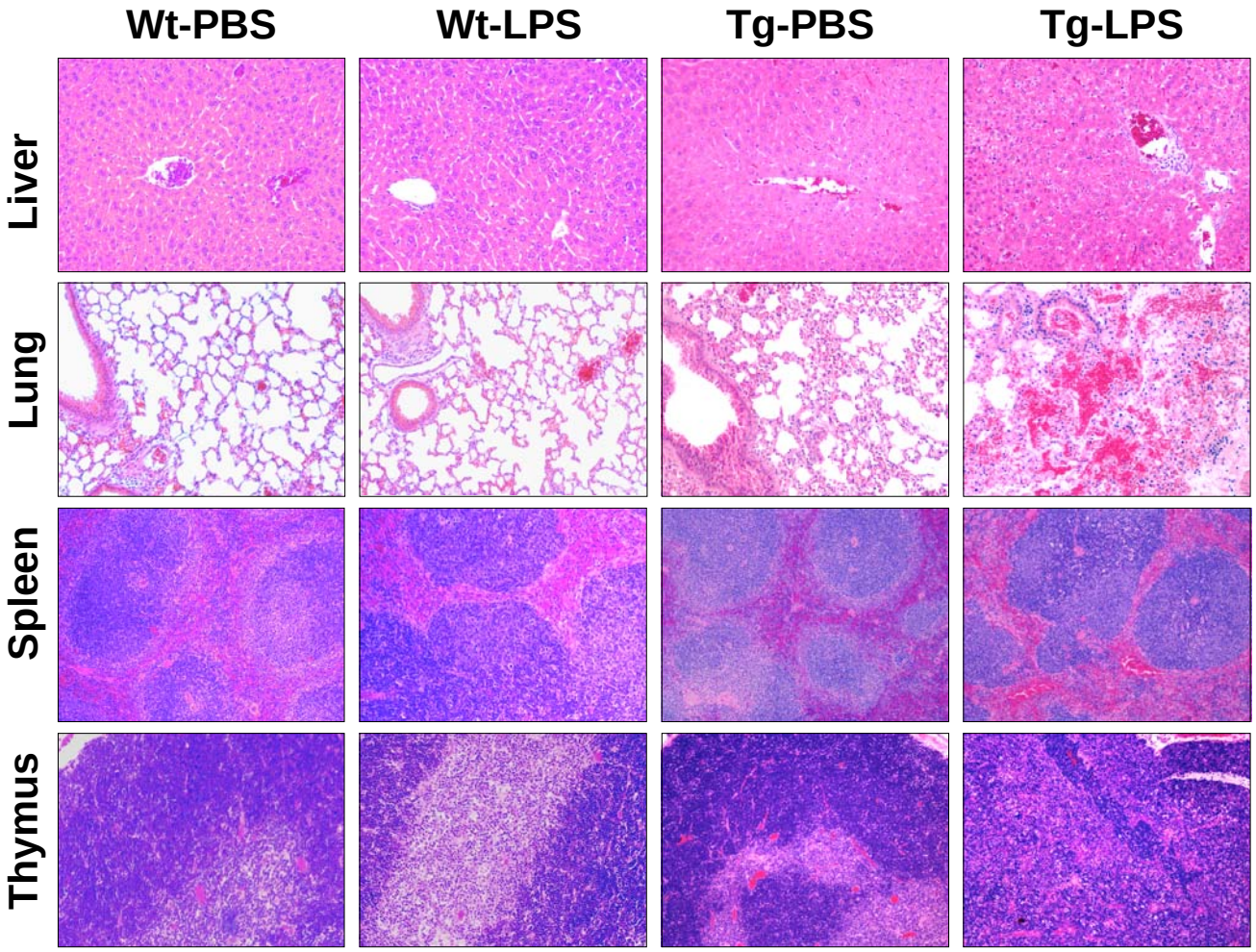

Fig. 2S-A

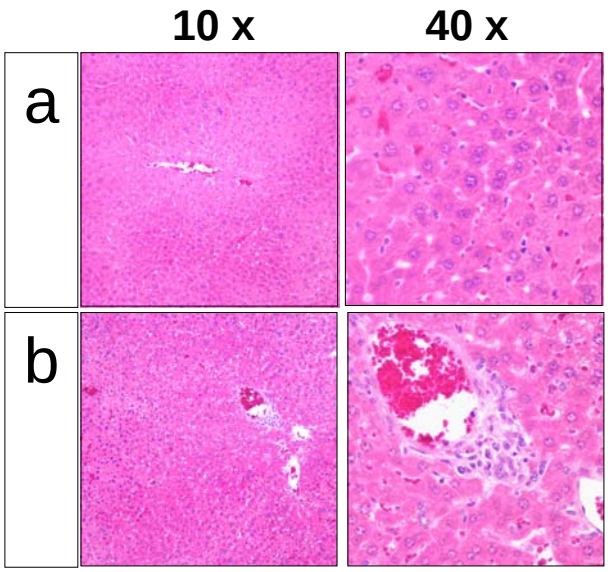

Fig. 2S-B

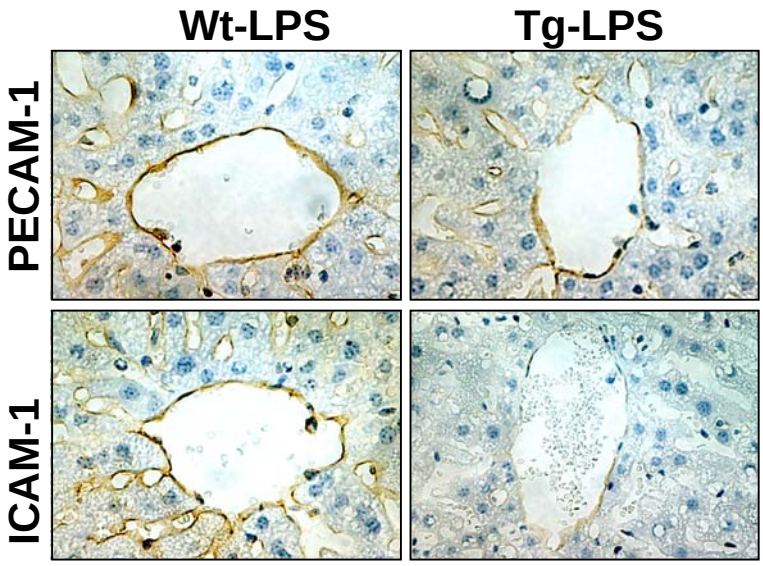

Fig. 2S-C

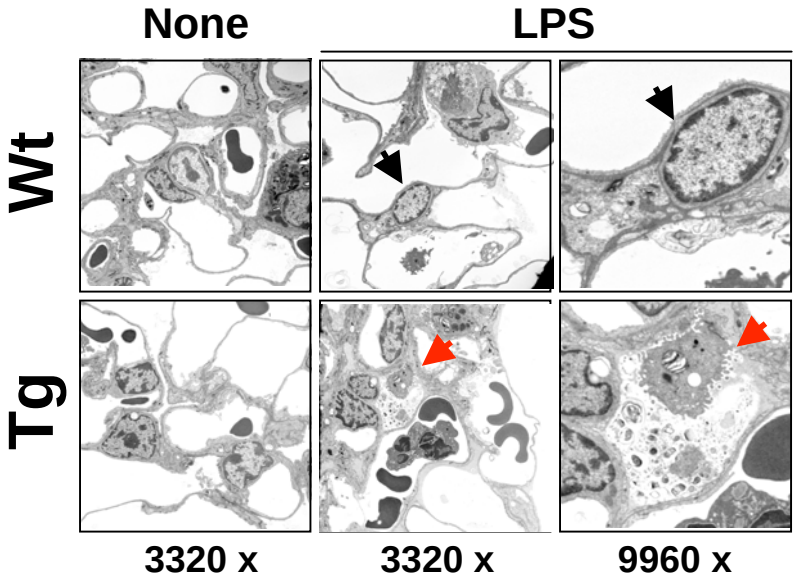

Fig. 3S-A

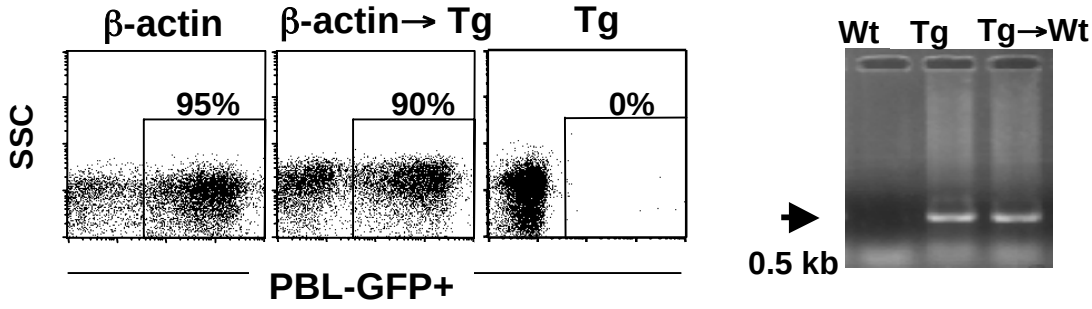

Fig. 3S-B

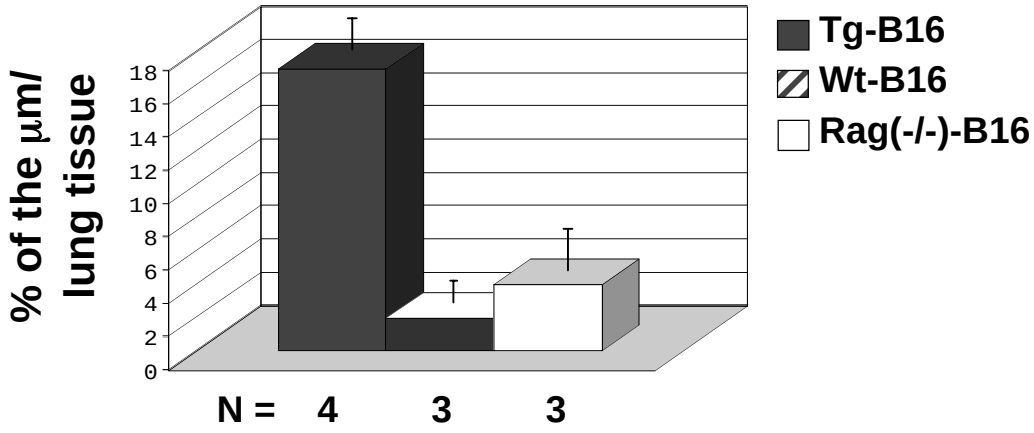

Fig. 3S-C

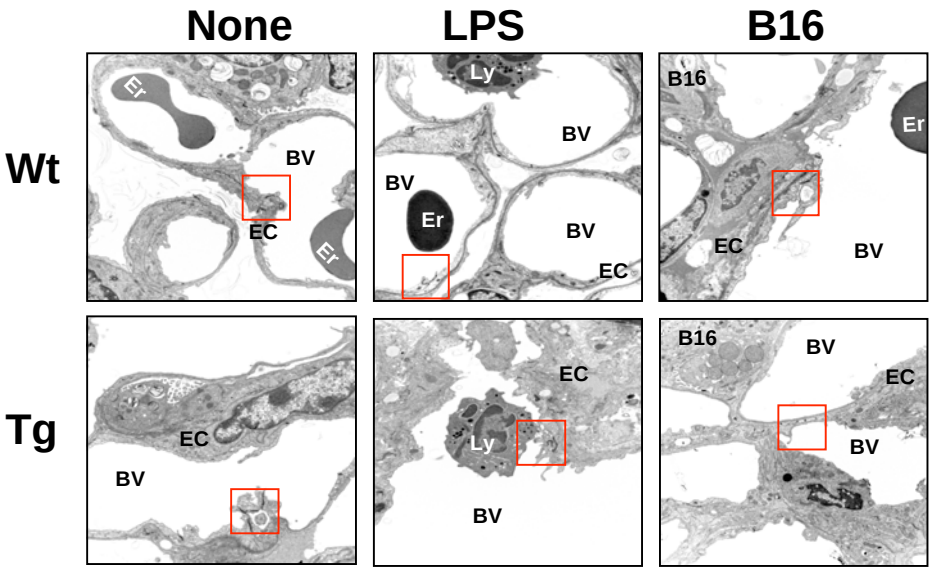

Supplementary Figures

Figure 1S. Genotype analysis of transgenic mice.

A. The offspring (F1) were examined by Southern blot analysis of the genomic tail DNA (digested with Hind III) and hybridized to the radiolabeled IκBα specific probe. Four transgenic lines were identified (i.e., Tie-Tg lines 1, 2, 3 and 4), which incorporated 16, 13, 18 and 21 copies of transgenic construct respectively. The transgene copy number was determined by comparison with the endogenous IkBα gene (2 copies), using a phosphoimager (Molecular Dynamics LabX, Midland, ON, Canada).

B. H & E stained tissues (Liver, Lung, Spleen and Thymus) from transgenic (Line 2) and wild type littermate control mice 18 h after injection with PBS or LPS (2 μg/g), as observed under a 10 X objective. Changes in Tie-Tg liver are notable for isolated liver infarcts and apoptotic hepatocytes. Periportal areas exhibit significant leukocyte infiltration and the loss of sinusoidal ECs. Changes in Tie-Tg lungs are notable for leukocytic infiltrates and hemorrhagic foci. Changes in Tie-Tg spleen are notable for expansion of the red pulp and significant evidence of apoptosis in white pulp. Changes in Tie-Tg thymus are notable loss of normal architecture and evidence of significant apoptosis. Similar results were obtained for Tie-Tg line 4.

Figure 2S. Histopathological analysis of tissues from LPS-challenged transgenic mice.

A. Post-mortem histological examination of two paraffin embedded hepatic samples (**a** and **b**) from a Tie-Tg mouse (line 2) treated with LPS (8 μg/g, 48 h). Analysis under 10 X and 40 X objectives revealed extensive liver damage, including evidence of hepatic necrosis, sinusoidal dilation, perivascular lymphocytic infiltration and endothelial hypertrophy.

B. Endothelial destruction in liver from LPS (IV; 2 μg/g, 24h) treated wild type (Wt) and transgenic mice (Tg), as revealed by immunostaining for PECAM-1

and ICAM-1, and visualized under a 40 X objective. ICAM-1 staining is prevalent (i.e., up regulated; data not shown) in wild type mice, but essentially absent in transgenic mice. Loss of ICAM-1 staining correlates directly with loss of PECAM-1^+ cells.

C. Endothelial apoptosis in lung from LPS (IV; 2 μg/g, 18h) untreated (None) and treated wild type (Wt) and transgenic mice (Tg; line 4) as revealed by EM (9960 X magnification). Normal and apoptotic nuclei are indicated by red and black arrows, respectively. Images are representative of the five 3320 X fields examined.

Figure 3S. Analysis of tumor B16-BL6 melanoma growth in mice.

A. Wild type (Wt) and transgenic (Tg) mice were engrafted with either transgenic or wild type (i.e., from β-actin–GFP mice) bone marrow (BM). FACS analysis of GFP expressing wild type BM (from β-actin→GFP transgenic mice; n = 4) revealed that $\geq$ 95 % by PBL were GPF^+. Engraftment of wild type mice with transgenic BM (Tg→Wt), evaluated by the PCR, was also found to be similarly efficient. Data includes mice from both transgenic lines 2 and 4.

B. Quantification of tumor burden (as percent area of total lung tissue) in transgenic (Tg; n = 4), wild type (Wt; n = 3) and Rag2-/- (n = 3) lungs. Tumor burden was modest, but similar in Rag2-/- (3 %) and wild type (1 %) mice when compared to Tie-Tg (15.6 %; $p < 0.005$). Results are indicated as the percent of the tumor expansion within 5 fields of lung tissue (in square μm ± SD).

C. Ultrastructural analysis of wild type (Wt) and Tie-Tg lung endothelium either before (None) or after LPS (2 μg/g, 18 h) treatment 2 weeks after B16-BL6 tumor injection (B16) evaluated by EM (3320 X) magnification. Red boxes indicate areas evaluated at higher magnification (i.e., 9960 X) fo2 tight junction morphology in Figure 6. Only one set of B16 injected 3320 X images are shown. Analysis includes both Tie-Tg lines 2 and 4.